



FACULDADE DE MEDICINA DA UNIVERSIDADE DE COIMBRA

TRABALHO FINAL DO 6º ANO MÉDICO COM VISTA À ATRIBUIÇÃO DO GRAU DE MESTRE NO ÂMBITO DO CICLO DE ESTUDOS DE MESTRADO INTEGRADO EM MEDICINA

MÁRIO LUÍS NÔRO LAÇO

INCREASED BRAIN LEVELS OF HYDROGEN
PEROXIDE IN A TRANSGENIC MOUSE MODEL OF
HUNTINGTON'S DISEASE

ARTIGO CIENTÍFICO

ÁREA CIENTÍFICA DE BIOQUÍMICA

TRABALHO REALIZADO SOB A ORIENTAÇÃO DE:
PROFESSORA DOUTORA ANA CRISTINA REGO

MARÇO 2015

INCREASED BRAIN LEVELS OF HYDROGEN PEROXIDE IN A TRANSGENIC MOUSE MODEL OF HUNTINGTON'S DISEASE

MÁRIO LUÍS NÔRO LAÇO

This work was partially funded by the Portuguese Foundation for Science and Technology, under the POPH and QREN programs (Post-doc Fellowship SFRH/BPD/91811/2012) and ‘Santa Casa Misericórdia de Lisboa’ (SCML) – Mantero Belard Neuroscience Award ‘13.

Este trabalho foi parcialmente financiado pela Fundação para a Ciência e a Tecnologia, através dos programas POPH e QREN (bolsa de pós-doutoramento com a referência SFRH/BPD/17275/2004) e pela Santa Casa da Misericórdia de Lisboa - Prémio Neurociências Mantero Belard 2013.



FACULDADE DE MEDICINA DA UNIVERSIDADE DE COIMBRA

MARÇO 2015

To my mother and my father.

À minha mãe e ao meu pai.

“sed etiam si cecidit de genu pugnat”

“but even he fell, he fights on his knees”

“e mesmo que caia, ele combate de joelhos”

(Lucius Annaeus Seneca, De Providentia, II, 6)

Table of contents

- Abbreviations.....5

**Increased brain levels of hydrogen peroxide in a transgenic mouse model of
Huntington’s disease**

- Abstract.....6

- Resumo.....8

- Introduction.....10

- Material and methods.....13

- Results.....18

- Discussion.....30

- Acknowledgments.....34

- References.....35

Abbreviations

ADP	Adenosine 5'-diphosphate monopotassium salt
ATP	Adenosine triphosphate
BSA	Bovine serum albumin
Ca ²⁺	Calcium
CCCP	Carbonyl cyanide m-chlorophenyl hydrazone
DH	Doença de Huntington
DNA	Deoxyribonucleic acid
EGTA	Ethylene glycol tetraacetic acid
FCCP	Carbonyl cyanide 4-trifluoromethoxy phenylhydrazone
H ₂ O ₂	Hydrogen peroxide ou peróxido de hidrogénio
HD	Huntington's disease
Htt	Huntingtin
IB	Isolation buffer
KHR	Krebs'-HEPES-Ringer's
polyQ	Polyglutamine
RCR	Respiratory control ratio
TMRM ⁺	Tetramethyl rhodamine methyl ester
ROS	Reactive oxygen species
SOD1	Superoxide dismutase 1
WT	Wild-type
YAC	Yeast artificial chromosome

Increased brain levels of hydrogen peroxide in a transgenic mouse model of Huntington's disease

Mário N. Laço^{1,2,3}, Sandra Mota¹, I. Luísa Ferreira¹, A. Cristina Rego^{1,3}

¹ Center for Neuroscience and Cell Biology

² Institute for Nuclear Sciences Applied to Health

³ Institute of Biochemistry, Faculty of Medicine; University of Coimbra, Coimbra, Portugal

Abstract

Huntington's disease (HD) is an inherited autosomal neurodegenerative disorder characterized by neuronal loss in specific brain regions, notably the striatum and the cortex. HD is associated with a dynamic mutation, an expansion in CAG repeats, located in the exon 1 of the *HD* gene. When the CAG expansion exceeds 35 repeats, progressive motor disability, including chorea and rigidity, cognitive impairment and psychiatric symptoms become apparent. The *HD* gene codes for a 350 kDa protein with still unknown function, huntingtin. The expanded CAG tract is translated into an elongated polyglutamine (polyQ) domain at the N-terminus of huntingtin. The polyQ domain confers mutated huntingtin with new cellular toxic properties and a higher propensity for protein aggregation. Several pathological mechanisms have been proposed for HD pathogenesis. Previous data suggested a contribution of oxidative stress in HD neurodegeneration, however the precise role of these mechanisms in HD are still not entirely understood. To clarify this role, we isolated cortical brain synaptosomes and mitochondria from YAC128 HD transgenic (expressing full-length human mutant huntingtin) and age-matched wild-type mice with 9 and 12 months of age. Oxygen consumption was evaluated in freshly isolated cortical synaptosomes and no differences were observed between YAC128 and wild-type mice, at 9 and 12 months of age. Moreover, wild-

type and HD synaptosomes exhibited similar intrasynaptosomal Ca^{2+} levels, even after exposure to hydrogen peroxide (H_2O_2 , 1 mM), a strong oxidant, or antimycin A (2 μM), a selective inhibitor of mitochondrial complex III. Concordantly, no differences in mitochondrial membrane potential were detected in HD and wild-type synaptosomes following exposure to H_2O_2 or antimycin A. However, HD synaptosomes at 12 months of age exhibited significantly higher basal levels of H_2O_2 . At 9 months of age, the increase in H_2O_2 levels observed in HD synaptosomes was only observed after a pre-incubation with H_2O_2 . Nevertheless, isolated cortical brain mitochondria from wild-type and YAC128 with 12 months of age exhibited no differences in H_2O_2 production at basal levels or after antimycin A or H_2O_2 stimuli. These data suggest a gradual increase in reactive oxygen species production following disease progression in YAC128 mice that may underlie cortical synaptic dysfunction.

Keywords: Huntington's disease, synaptosomes, mitochondria, oxidative stress, YAC128 mice.

Resumo

A doença de Huntington (DH) é uma patologia neurodegenerativa, hereditária, autossômica, dominante, caracterizada pela perda neuronal em regiões cerebrais específicas, nomeadamente no estriado e no córtex. A DH está associada à expansão dinâmica de repetições do codão CAG no exão 1 do gene *HD* que codifica para uma proteína de 350 kDa, de função ainda desconhecida, a huntingtina. Quando a expansão de CAG ultrapassa as 35 repetições surgem sintomas psiquiátricos, incapacidade motora progressiva, incluindo coreia e rigidez, e défice cognitivo. A expansão de CAGs é transcrita como um domínio aumentado de poliglutaminas no terminal amínico da huntingtina. A expansão de poliglutaminas confere à huntingtina mutante novas propriedades celulares, tóxicas e uma maior propensão para a agregação proteica. Vários mecanismos patológicos têm sido propostos para a patogénese da DH. Trabalhos anteriores sugerem uma contribuição do stresse oxidativo na neurodegenerescência que ocorre na DH, contudo o papel definitivo destes mecanismos ainda não estão totalmente esclarecidos. Para clarificar este papel, foram isolados sinaptossomas e mitocôndrias cerebrais a partir de murganhos “wild-type” e transgênicos para a DH (YAC 128), com 9 ou 12 meses de idade. O consumo de oxigénio foi avaliado em sinaptossomas corticais frescos, contudo não foram observadas diferenças entre murganhos “wild-type” e YAC128, tanto aos 9 como aos 12 meses de idade. Mais ainda, os sinaptossomas normais e DH apresentaram níveis semelhantes de Ca^{2+} intracelular, mesmo após a estimulação com peróxido de hidrogénio (H_2O_2 - 1 mM), um forte oxidante; ou com antimicina A (2 μM), um inibidor seletivo do complexo mitocondrial III. Em concordância, também não foram detetadas diferenças no potencial mitocondrial transmembranar dos sinaptossomas “wild-type” e sinaptossomas DH, após a exposição a H_2O_2 ou antimicina A. Contudo, os sinaptossomas de YAC128 com 12 meses apresentaram níveis basais de H_2O_2 significativamente mais elevados. Aos 9 meses de idade, o aumento dos níveis de H_2O_2 pelos sinaptossomas DH só foi observado após a pré-incubação com H_2O_2 . Todavia, mitocôndrias cerebrais isoladas a partir de murganhos “wild-

type” ou YAC128 com 12 meses de idade não mostraram diferenças na produção basal de H_2O_2 , ou mesmo, após estimulação com antimicina A ou H_2O_2 . Estes resultados sugerem que existe um aumento gradual na produção de espécies reativas de oxigênio, associada à progressão da doença nos murganhos YAC128, que pode indicar a ocorrência de uma disfunção sináptica cortical.

Palavras-chave: Doença de Huntington, sinaptossomas, mitocôndria, stresse oxidativo, murganhos transgênicos YAC128.

Introduction

Huntington's disease (HD) is an inherited autosomal dominant neurodegenerative disorder with a worldwide prevalence of 5 to 10 patients per 100,000 people, affecting both men and women equally.¹⁻³ Neurodegeneration is more evident in the striatum and the cortex, however the hippocampus, the *substantia nigra* and the thalamus also show signs of degeneration, as disease progresses.^{4,5}

HD is characterized by abnormal, uncoordinated, involuntary (choreic or “dance-like”) movements. The first symptoms usually become apparent between the third and the fifth decade of life, although alterations in behaviour, emotional disturbances, psychiatric symptoms and deficits in cognition may be detected decades before the onset of motor signs.⁶⁻

¹⁰ Later on, HD patients might exhibit bradykinesia, ataxia, rigidity, dystonia (symptoms also observed in juvenile cases), and cognitive impairment culminating in dementia.¹¹⁻¹⁶

Ultimately, HD is a fatal disease and death predictably occurs 15-20 years after the first symptoms. The causes of death include complications such as heart failure, physical injuries from falls, inanition, dysphagia and aspiration pneumonia.¹⁷

The genetic mutation associated with HD is an expansion in the number of CAG repeats in the exon 1 of the *HTT* gene, which codes for a protein of approximately 350 kDa with unknown physiological function, huntingtin (Htt)¹⁸. Healthy individuals have a CAG tract length spanning from 10 to 35 repeats, with HD symptoms becoming apparent when the CAG expansion exceeds 35 repeats¹⁹. The CAG codon codifies for the amino acid glutamine, thus the CAG expansion is translated into a polyglutamine (polyQ) domain located at the Htt N-terminus. The expanded polyQ domain destabilizes Htt, increases its propensity for aggregation and endows mutant Htt with new and toxic properties. Expression of mutant Htt has been associated with several pathological mechanisms, including excitotoxicity, apoptotic cell death, alterations in intracellular calcium-handling, transcription deregulation,

mitochondrial dysfunction and oxidative stress, the later associated to unbalanced antioxidant activity and free radical generation.²⁰⁻²³

Mitochondrial dysfunction has gained a central role in HD; interestingly, the striatum is a brain area highly susceptible to alterations in mitochondrial oxidative phosphorylation.^{24,25} Mitochondrial complex II activity seems to be reduced in the striatum of HD brains, and the administration of complex II inhibitors mimic the HD phenotype in animal and cell models of this disease.²⁶ Mitochondria from lymphoblasts of HD patients exhibited a lower mitochondrial potential and disruption of this potential at lower Ca^{2+} loads.^{27,28} Isolated mitochondria incubated with polyQ proteins revealed increased reactive oxygen species (ROS) production and a reduction in Ca^{2+} storage capacity.²⁹ The balance between ROS and antioxidants is also altered in HD. Fibroblasts from HD patients and HD cybrids exhibited higher mitochondrial ROS formation.^{30,31} Significant increases in markers of deoxyribonucleic acid (DNA) and protein oxidation were also observed in the striatum, cortex, serum, cerebrospinal fluid, leukocytes and in plasma of HD patients.^{23,32-40} Oxidation of mitochondrial enzymes was also reported in striatal samples of HD patients⁴¹. Furthermore, antioxidant systems are reduced in plasma and erythrocytes of HD patients.²³ Uric acid and glutathione levels (potent antioxidants) are reduced in HD patients, collectively with a reduction in catalase and superoxide dismutase 1 (SOD1 or Cu/Zn-SOD).^{33,42-44}

All together, these data suggest a major role of oxidative stress and mitochondrial dysfunction in HD, however, their precise contribution for HD pathogenesis and disease progression is still not entirely clear. To clarify this point, cortical synaptosomes and cortical mitochondria were isolated from wild-type mice and HD transgenic mouse model expressing full-length human mutant Htt with 128 CAG repeats, the YAC128 mice. YAC128 mice exhibit a robust phenotype and are commonly used as preclinical models in HD.⁴⁵ The levels of ROS and mitochondrial function were measured at different post-symptomatic stages of disease progression in the YAC128 mice, at 9 and 12 months of age, in order to assess the

mitochondrial dysfunction and oxidative stress associated to each stage of HD progression. The disease is phenotypically and neuropathologically established in YAC128 mice of 9 and 12 months, however cortical degeneration is only evident at the later age.⁴⁵

Material and methods

Material - Succinate, glucose, fatty acid free bovine serum albumin (BSA), adenosine 5'-diphosphate monopotassium salt (ADP), oligomycin, carbonyl cyanide m-chlorophenyl hydrazone (CCCP), carbonyl cyanide 4-trifluoromethoxy phenylhydrazone (FCCP), hydrogen peroxide (H₂O₂) and antimycin A were purchased from Sigma Aldrich (St. Louis, MO, USA). Fura-2/AM and tetramethyl rhodamine methyl ester (TMRM⁺) were obtained from Molecular Probes/Invitrogen (Eugene, OR, USA). Bio-Rad Protein Assay was from Bio-Rad (Hemel Hempstead, UK).

Animals - YAC128 mouse model of HD (expressing full-length human mutant huntingtin) was provided by Dr. Michael Hayden (University of British Columbia, Vancouver, Canada). The animals were housed at the Center for Neuroscience and Cell Biology (CNC)/Faculty of Medicine (University of Coimbra) animal facilities in controlled-temperature room and maintained on 12h light/dark cycle. Food and water were available *ad libitum*. The selection of heterozygous YAC128 and age-matched wild-type (WT) mice littermates with 9 and 12 months of age was based on animal genotyping using common molecular biology procedures. The animals were euthanized by cervical dislocation with all efforts being made to reduce animal suffering. The studies were performed according to Directive 2010/63/EU on the protection of animals used for scientific purposes.

Isolation of synaptosomes - The isolation of cortical nerve terminals was prepared using a combined sucrose/Percoll centrifugation protocol previously described.⁴⁶ Briefly, both cortices from brains of wild-type or YAC128 mice with 9 or 12 months of age were homogenized in a medium containing 0.32 M sucrose, 0.2 mM EDTA, and 5 mM HEPES-

Tris, pH 7.4. The homogenate was spun for 10 min at 2000 x *g* at 4°C and the supernatant spun again at 14,000 x *g* for 12 min. The pellet (P2 fraction) was resuspended in 1 ml of 45% Percoll (v/v) in Krebs'–HEPES–Ringer's (KHR) medium (140 mM NaCl, 1 mM EDTA, 5 mM KCl, 5 mM glucose and 10 mM HEPES, pH 7.4) and spun again at 14,000 x *g* for 2 min. Synaptosomes were then removed from the top layer, washed twice with KHR medium, and resuspended in a Krebs' solution (124 mM NaCl, 3 mM KCl, 1.25 mM NaH₂PO₄, 25 mM NaHCO₃, 2 mM MgSO₄, 2 mM CaCl₂, and 10 mM glucose).

Brain mitochondria isolation - YAC128 mice at 9 or 12 months of age and age-matched wild-type mice were sacrificed by cervical dislocation and the cortices were excised and immediately placed into ice-cold isolation buffer (IB) (225 mM mannitol, 75 mM sucrose, 1 mM EGTA, 5 mM HEPES–KOH, pH 7.2, 1 mg/mL BSA). Brain mitochondria were isolated using a discontinuous Percoll density gradient centrifugation previously described.⁴⁷ Shortly, the two cortices were dissected out and each cortex was homogenized separately in a 1-mL tissue grinder (Thomas Scientific, Swedesboro, NJ, USA) in 1 mL IB. Another 1 ml IB was added to the homogenate bringing the total volume to 2 ml. The homogenates derived from the two cortices of the same mice were combined and centrifuged briefly at 1100 x *g*, for 2 min, at 4°C. The supernatant was divided into five Eppendorf tubes with a final volume of 700 µL each and mixed with 75 µL of freshly made 80% Percoll (80 vol% Percoll diluted in 1 M sucrose, 50 mM HEPES, 10 mM EGTA, pH 7.0). Then, the mixtures were carefully layered on the top of freshly made 10% Percoll (750 µL, 80% Percoll was diluted in IB to prepare the 10% solution) in a 2 mL Eppendorf tube and centrifuged at 18 500 x *g*, for 10 min, 4°C. The cloudy myelin-containing top fractions were removed, leaving the mitochondria-enriched pellet in the bottom of the Eppendorf tubes. One milliliter sucrose washing buffer [sucrose washing buffer: 250 mM sucrose, 5 mM HEPES–KOH (pH 7.2), 0.1

mM EGTA] was added to the pellet, mixed, and centrifuged at 10 000 x g, for 5 min, at 4°C. The final mitochondrial pellet was resuspended in reaction buffer (100 mM sucrose, 100 mM KCl, 2 mM KH₂PO₄, 5 mM HEPES, 10 μM EGTA, pH 7.4) and retained on ice until used for further analysis.

Measurement of synaptosomal and mitochondrial H₂O₂ levels - H₂O₂ levels were measured by following Amplex red fluorescence (570 nm excitation, 585nm emission) at 30°C, for 15 min, using a Microplate Spectrofluorometer Gemini EM (Molecular Devices, USA). Wild-type and YAC128 cortical synaptosomes were resuspended in experiment buffer (132 mM NaCl, 1 mM KCl, 1 mM CaCl₂, 1.4 mM MgCl₂, 10 mM glucose, 10 mM HEPES-Tris, pH 7.4) containing Amplex red and horseradish peroxidase. Wild-type and YAC128 cortical mitochondria were maintained in reaction buffer (100 mM sucrose, 100 mM KCl, 2 mM KH₂PO₄, 5 mM HEPES, 10 μM EGTA) containing 10 μM Amplex red plus 0.5 U/ml horseradish peroxidase and enriched with 3 mM succinate to energize the mitochondria. 2 μM antimycin A was added to the synaptosomal or mitochondrial samples tested for inhibition of mitochondrial complex III. The stimulation with H₂O₂ consisted in a pre-incubation with 1 mM H₂O₂, for 30 min. Then, the synaptosomes or mitochondria were briefly washed to eliminate the residual H₂O₂, before recording the Amplex red fluorescence.

TMRM⁺ fluorescence - Mitochondrial membrane potential was assessed using the cationic fluorescent probe TMRM⁺, which accumulates predominantly in polarized mitochondria. Thus, the variation of TMRM⁺ retention was studied in order to estimate changes in mitochondrial membrane potential. Following a washing step, wild-type and YAC128 cortical synaptosomes were incubated in loading buffer (132 mM NaCl, 1 mM KCl, 0.1 mM CaCl₂, 1.4 mM MgCl₂, 10 mM glucose, 10 mM HEPES-Tris, pH 7.4) containing 300 nM TMRM⁺

(quench mode) for 30 min at 30°C. After loading, the synaptosomes were transferred to experiment buffer (132 mM NaCl, 1 mM KCl, 1 mM CaCl₂, 1.4 mM MgCl₂, 10 mM glucose, 10 mM HEPES-Tris, pH 7.4) and their basal fluorescence (540 nm excitation and 590 nm emission) was measured using a microplate reader Spectrofluorometer Gemini EM (Molecular Devices, USA), for 5 min, followed by the addition of 2 μM FCCP plus 2 μg/mL oligomycin to produce maximal mitochondrial depolarization. 2 μM antimycin A and 1 mM H₂O₂ stimuli were administered after 5 min of basal recording and before the mitochondrial depolarization with FCCP/oligomycin.

Intrasynaptosomal Ca²⁺ recordings - Wild-type and YAC128 cortical synaptosomes were incubated in loading buffer (132 mM NaCl, 1 mM KCl, 0.1 mM CaCl₂, 1.4 mM MgCl₂, 10 mM glucose, 10 mM HEPES-Tris, pH 7.4) containing 5 μM Fura-2/AM the fluorescent probe at 30° C, for 30 min. After a washing step, intrasynaptosomal Ca²⁺ levels were measured in experiment buffer (132 mM NaCl, 1 mM KCl, 1 mM CaCl₂, 1.4 mM MgCl₂, 10 mM glucose, 10 mM HEPES-Tris, pH 7.4) under basal conditions or in response to 1 mM H₂O₂ or 2 μM antimycin A and 2 μM FCCP plus 2 μg/mL oligomycin, using a Spectrofluorometer Gemini EM (Molecular Devices, USA), with 340/380 nm excitation and 510-nm emission wavelengths.

O₂ consumption - Wild-type and YAC128 cortical synaptosomes were resuspended in experiment buffer (132 mM NaCl, 1 mM KCl, 1 mM CaCl₂, 1.4 mM MgCl₂, 10 mM glucose, 10 mM HEPES-Tris, pH 7.4), while wild-type and YAC128 cortical mitochondria were diluted in reaction buffer (100 mM sucrose, 100 mM KCl, 2 mM KH₂PO₄, 5 mM HEPES, 10 μM EGTA). Cortical synaptosomes or mitochondria were placed in an oxygen electrode chamber (DW1, Clark electrode, Hansatech, UK), after calibration for dissolved oxygen. The

basal rate of oxygen consumption (in $\text{nmol mL}^{-1} \text{min}^{-1}$) of synaptosomes was recorded for 2 minutes, at 30 °C, after which it was assessed the maximum respiration by adding 2 $\mu\text{g/mL}$ oligomycin followed by 2 μM CCCP. KCN (700 μM) was added at the end of the experiment to confirm O_2 consumption. The mitochondria were energized with 3 mM succinate and their basal rate of oxygen consumption recorded at 30 °C. Then, they were challenged by two independent boots of 25 nM ADP, followed by 2 $\mu\text{g/mL}$ oligomycin and 2 μM CCCP stimuli. KCN (700 μM) was added at the end of the experiment to confirm O_2 consumption by mitochondria.

Data Analysis and Statistics - Data were expressed as the mean \pm SEM of the number of experiments indicated in the figure legends. Comparisons among multiple groups were performed by two-way ANOVA, followed by Sidak's multiple comparisons test. Student's t test was also performed for comparison between two Gaussian populations, as described in figure legends. Significance was accepted at $p < 0.05$.

Results

YAC128 synaptosomes show an age-associated increase in H₂O₂ production

The main aim of this study was to understand the relevance of oxidative stress in HD. We initiated our work by measuring the levels of hydrogen peroxide (H₂O₂), a potent oxidant, in cortical synaptosomes from wild-type and YAC128 mice with 9 or 12 months of age. The rate of H₂O₂ production was determined using Amplex red reagent.

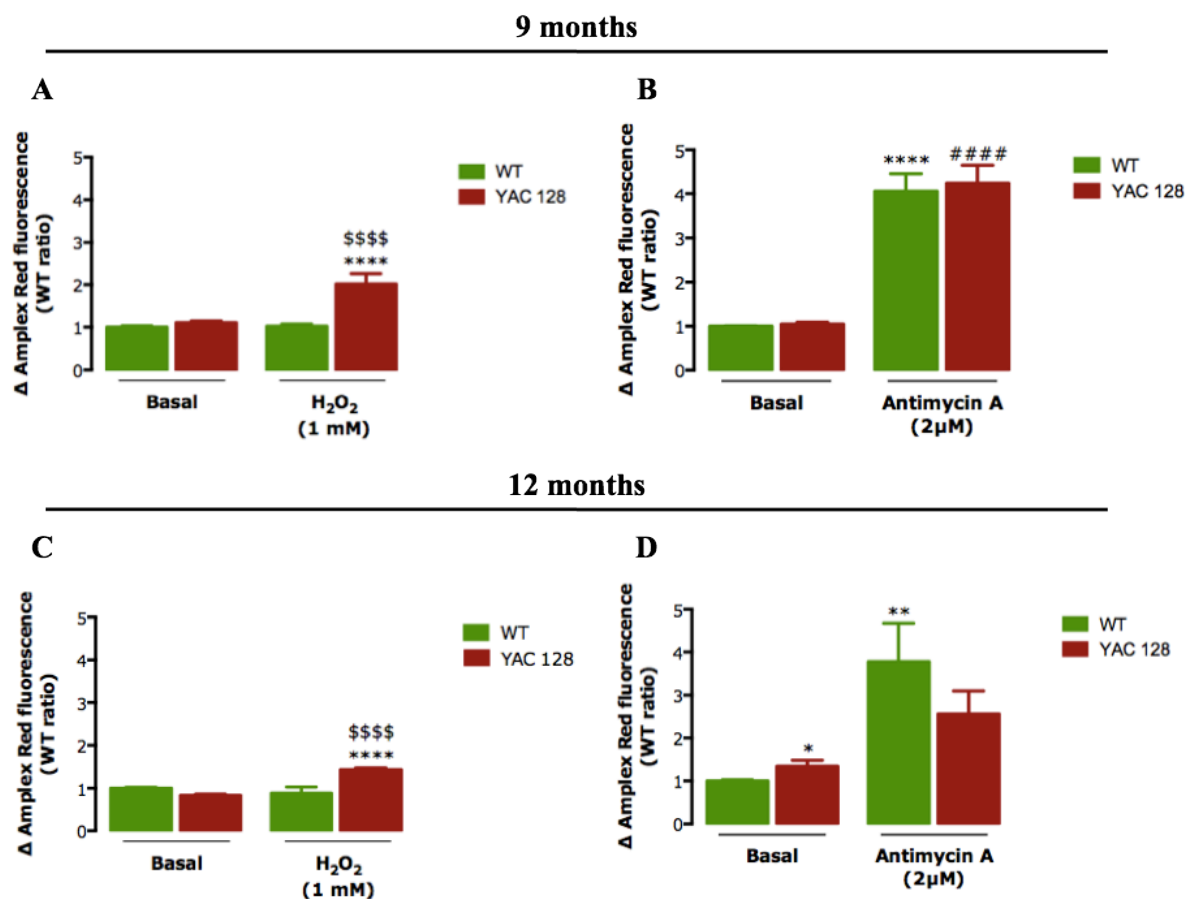


Figure 1. YAC128 synaptosomes show an increase in H₂O₂ levels under an oxidative environment.

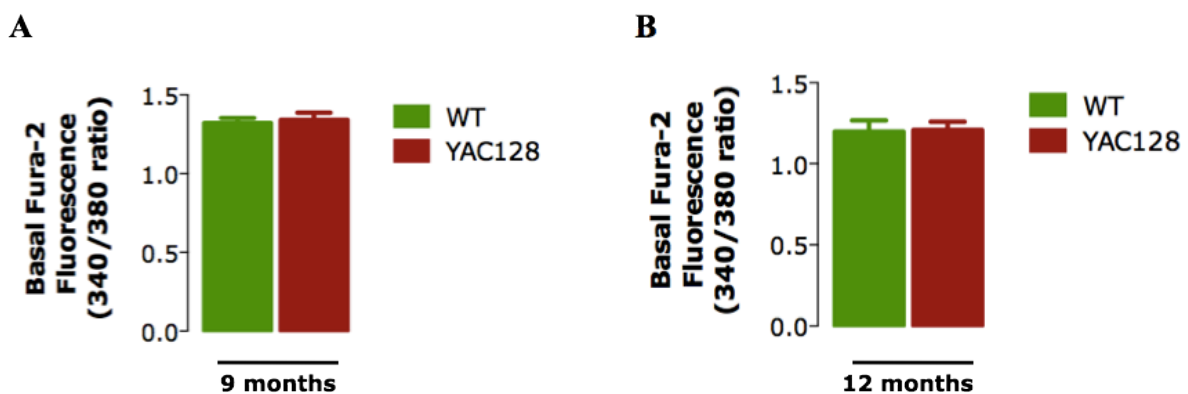
The production of H₂O₂ was measured in wild-type and YAC128 cortical synaptosomes from mice at 9 (A, B) or 12 (C, D) months of age. The increase in H₂O₂ levels was assessed under basal conditions, after a 2 μM antimycin A stimulus (B, D) or 30 min pre-incubation with 1 mM H₂O₂ (A, C), through Amplex red fluorometry. Data are the mean ± S.E.M. of 4 independent experiments performed in triplicates or quadruplicates. Statistical analysis: ****P<0.0001 compared to wild-type basal conditions, ssssP<0.0001 compared to H₂O₂-treated wild-type, #####P<0.0001 compared to YAC128 basal conditions, **P<0.01 compared to wild-type basal conditions (two-way ANOVA, followed by Sidak's multiple comparisons test), *P<0.05 compared to wild-type basal conditions (Student's *t*-test).

Freshly isolated synaptosomes were incubated in Amplex red containing medium and the increase in fluorescence was followed for a 15 minutes period. To study the levels of H₂O₂ in stressfully challenged mitochondria, some samples were incubated with 2 μM antimycin A, a selective inhibitor of mitochondrial complex III, while other samples were pre-incubated with 1 mM H₂O₂ for 30 min, to mimic a highly oxidative environment.

Under basal conditions, wild-type and YAC128 cortical synaptosomes from 9 month-old mice did not show any difference in the levels of H₂O₂ (Fig. 1A,B). However, cortical synaptosomes from 12 month-old YAC128 mice exhibited significantly higher basal levels of H₂O₂, prior to any stimulus (Fig. 1D). As could have been predicted, both stimuli produced some increase in H₂O₂ levels in wild-type and YAC128 synaptosomes (Fig. 1), although mitochondrial inhibition with antimycin A showed a higher and more consistent effect, in comparison to the pre-incubation with H₂O₂ (Fig. 1B,D). Nonetheless, the incubation with antimycin A did not produce statistically different increases in H₂O₂ levels between wild-type and YAC128 synaptosomes, either at 9 or 12 months of age (Fig. 1B,D). On the other hand, pre-incubation with H₂O₂ only seem to predispose YAC128 synaptosomes to a higher production of H₂O₂, since only these synaptosomes demonstrated a statistically significant increase in H₂O₂ levels, after the stimulus, at both ages tested (Fig. 1A,C). Moreover, this increase in H₂O₂ was statistically different from wild-type levels, both at 9 and 12 months (Fig. 1A,C).

YAC128 and wild-type cortical synaptosomes have similar basal levels of intrasynaptosomal Ca²⁺ at 9 and 12 months

In previous works, HD cell and animal models have shown a deregulation of intracellular Ca²⁺ handling.²⁷⁻²⁹ Therefore, we ought to evaluate if there was any difference in basal intracellular Ca²⁺ in our model, prior to any given stimuli, that could relate to the increase in H₂O₂ production previously observed. Cortical synaptosomes from YAC128 and wild-type mice with 9 and 12 months of age were isolated and loaded with Fura2-AM, a high affinity intracellular ratiometric fluorescent Ca²⁺ probe. Since Fura2-AM is a ratiometric Ca²⁺ indicator, one can compare directly the relative intracellular Ca²⁺ levels between samples. Surprisingly, YAC128 and wild-type synaptosomes had similar basal intrasynaptosomal Ca²⁺ levels, both at 9 and 12 months (Fig. 2). Moreover, the values between different ages were comparable, suggesting that the aging process was not affecting the intrasynaptosomal Ca²⁺



levels (Fig.2A,B).

Figure 2. No differences in basal intrasynaptosomal Ca²⁺ levels between wild-type and YAC128 synaptosomes.

Fura2-AM fluorescence was analysed in wild-type and YAC 128 cortical synaptosomes from mice with 9 (A) or 12 (B) months. Basal Ca²⁺ levels were assessed through the calculation of Ca²⁺-bound Fura2 (340 nm)/ Ca²⁺-unbound Fura2 (380 nm) fluorescence ratio. Data are the mean \pm S.E.M. of 4 independent experiments performed in triplicates to quadruplicates.

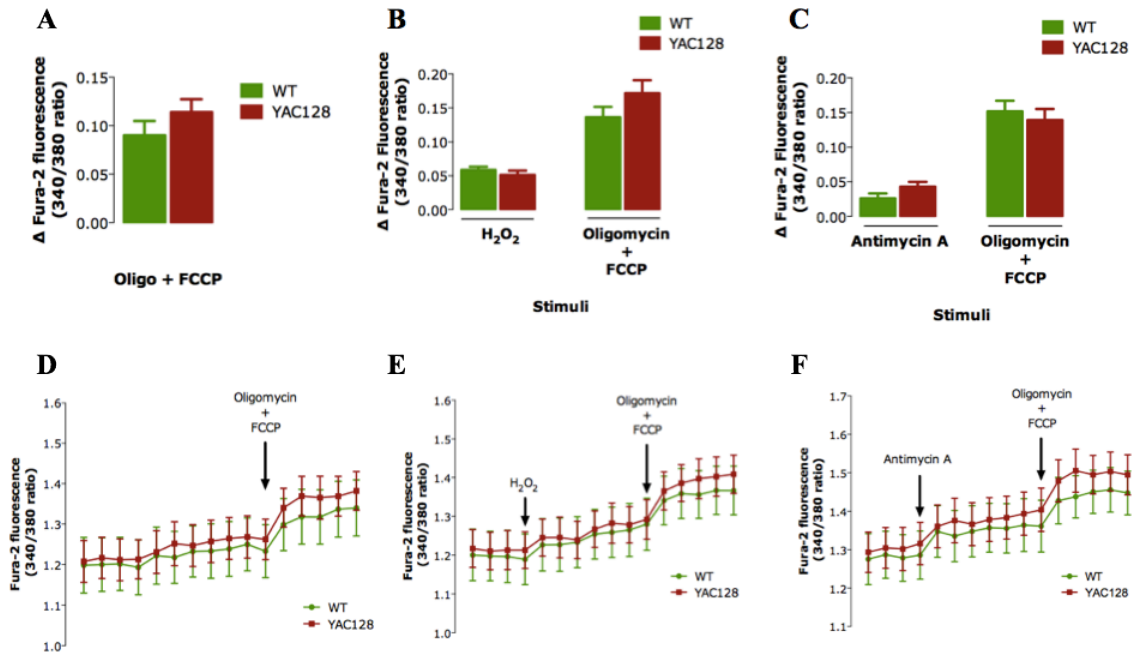
No differences in the intrasynaptosomal Ca²⁺ responses of wild-type or YAC128 synaptosomes to mitochondrial/oxidative stress stimuli

Since YAC128 and wild-type synaptosomes had no differences at the basal intrasynaptosomal Ca²⁺ levels, we tested whether these two populations of synaptosomes behaved similarly under stressful conditions, in an attempt to uncover differences in intrasynaptosomal Ca²⁺ responses between wild-type and YAC128. Antimycin A, a selective inhibitor of mitochondrial complex III, was used to produce a mitochondrial-directed insult, while the administration of H₂O₂ high levels of oxidative stress.

Complete depolarization of mitochondrial potential with 2µg/ml oligomycin (an adenosine triphosphate (ATP) synthase inhibitor) and 2 µM FCCP (a protonophore) induced an expected increase in cytoplasmic Ca²⁺ levels due to the release of Ca²⁺ from mitochondrial stores. No differences were observed between wild-type and YAC128 cortical synaptosomes in the oligomycin/FCCP-induced intrasynaptosomal Ca²⁺ increase, both at 9 and 12 months (Fig. 3A, 3D, 3G, 3J), indicating that mitochondria from wild-type and YAC128 synaptosomes have a similar Ca²⁺ buffering capacity at both ages tested.

Accordingly, wild-type and YAC128 cortical synaptosomes exhibited similar intrasynaptosomal Ca²⁺ increases in response to 2 µM antimycin A (Fig. 3C, 3F, 3I, 3L) or 1 mM H₂O₂ (Fig. 3B, 3E, 3H, 3K). The only remark is the difference in response to antimycin A inhibition by the synaptosomes of different ages. At 9 months, antimycin A induces a smaller intrasynaptosomal Ca²⁺ increase, when compared to synaptosomes of 12 months of age (Fig. 3C, 3I). However, both wild-type and YAC128 synaptosomes exhibit this pattern of response to antimycin A, with no differences observed between the two populations of synaptosomes at each age.

9 months



12 months

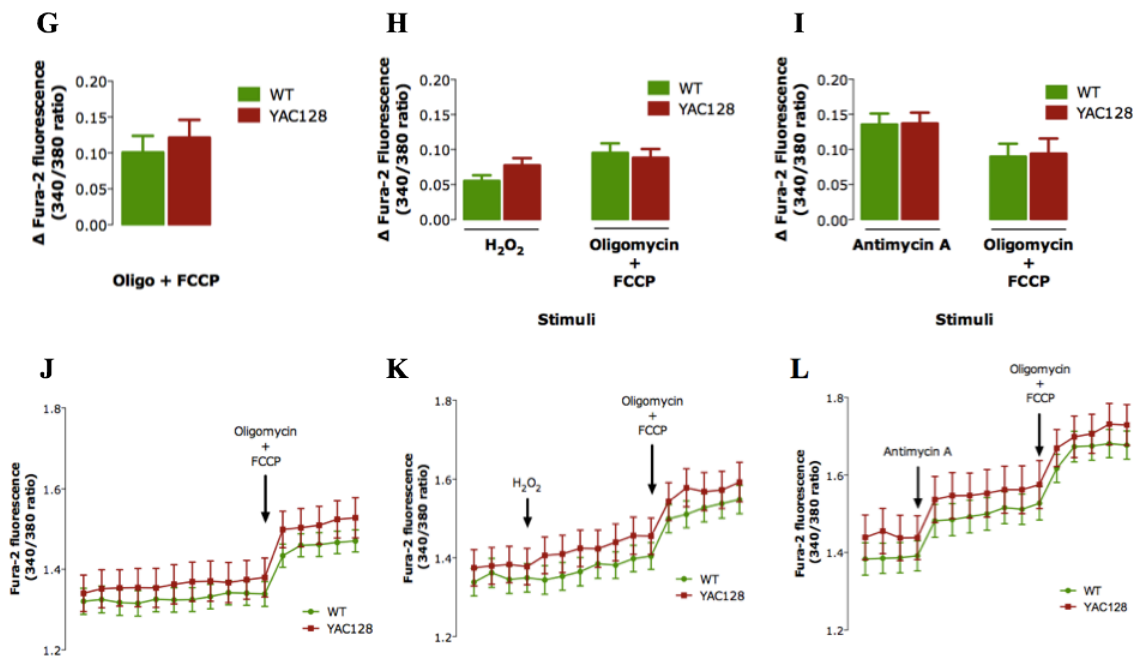


Figure 3. No differences in intrasynaptosomal Ca²⁺ levels between wild-type or YAC128 synaptosomes. Fura2-AM fluorescence was analysed in wild-type and YAC 128 cortical synaptosomes from mice with 9 (A, B, C, D, E, F) or 12 (G, H, I, J, K, L) months. Basal Ca²⁺ levels were obtained after complete mitochondrial membrane depolarization with of 2 μ M FCCP plus 2 μ g/ml oligomycin (A, D; G, J). Ca²⁺ levels were also measured after 2 μ M antimycin A (C, F, I, L) or 1 mM H₂O₂ (B, E, H, K) stimulus, followed by complete mitochondrial depolarization with FCCP + oligomycin. Results were expressed as the increase in Fura2 ratio after the stimulus (A, B, C, G, H, I). Graphs are representative registers of intrasynaptosomal Ca²⁺ levels through time, during the experiments (D, E, F, J, K, L). Data are the mean \pm S.E.M. of 4 independent experiments performed in triplicates to quadruplicates.

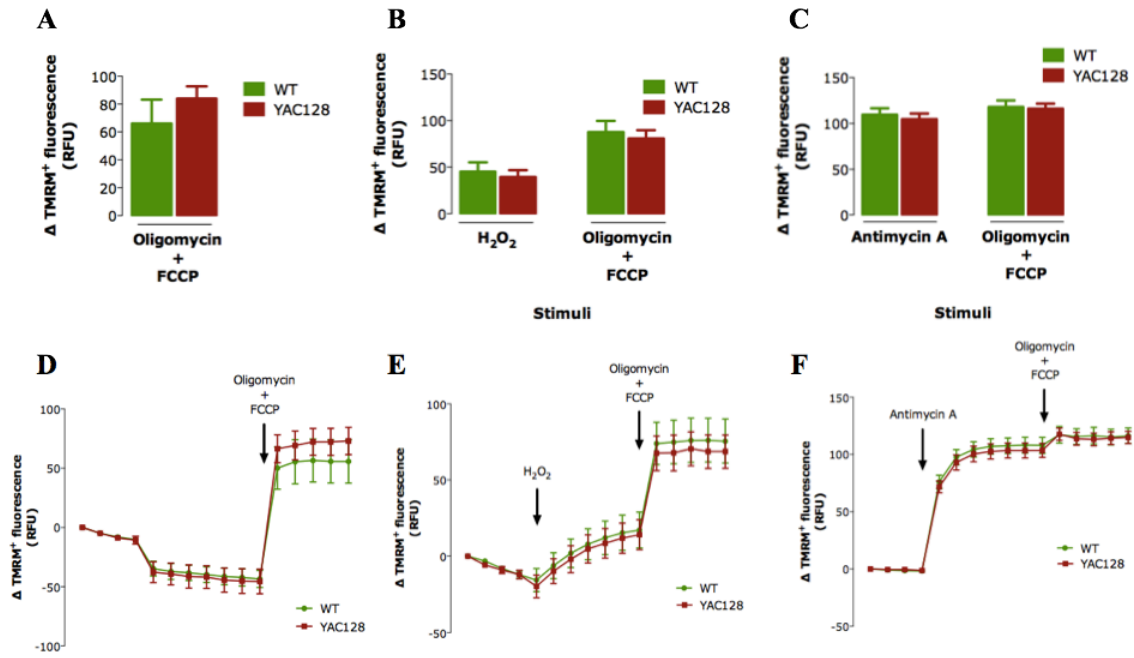
Moreover, at 12 months, both wild-type and YAC128 cortical synaptosomes seem to have less available Ca^{2+} in mitochondrial stores, after a prior stress stimulus, when compared with 9-month synaptosomes, since the final oligomycin/FCCP mitochondrial depolarizations in 12-month synaptosomes produced smaller intrasynaptosomal Ca^{2+} releases (Fig. 3B, 3C, 3H, 3I).

Mitochondrial inhibition and oxidative stress stimuli produce comparable alterations in mitochondrial potential of wild-type and YAC128 cortical synaptosomes

Simultaneously to the assessment of intrasynaptosomal Ca^{2+} levels, the alterations in mitochondrial potential of wild-type and YAC128 cortical synaptosomes were also evaluated in the same set of experiments. To achieve this, wild-type and YAC128 synaptosomes were loaded with TMRM⁺, a cationic fluorescent probe, which readily accumulates inside mitochondria in a mitochondrial potential-dependent manner. Inside mitochondria, TMRM⁺ reaches such high concentrations that its fluorescence is quenched. Therefore, a reduction in mitochondrial potential promotes the exit of TMRM⁺ molecules out of the mitochondria, which is translated into a dequenching of TMRM⁺ fluorescence and a rapid increase in its signal.

As expected, the addition of 2 $\mu\text{g}/\text{ml}$ oligomycin and 2 μM FCCP produced an increase in TMRM⁺ fluorescence, since FCCP, being a protonophore, promotes the depolarization of mitochondrial potential (Fig 4A, 4D, 4G, 4J). Even so, wild-type and YAC128 cortical synaptosomes showed no differences in the increase of TMRM⁺ fluorescence after complete mitochondrial depolarization with oligomycin plus FCCP, either at 9 or 12 months, suggesting that mitochondria from wild-type and YAC128 synaptosomes are able to develop similar mitochondrial potentials (Fig 4A, 4G).

9 months



12 months

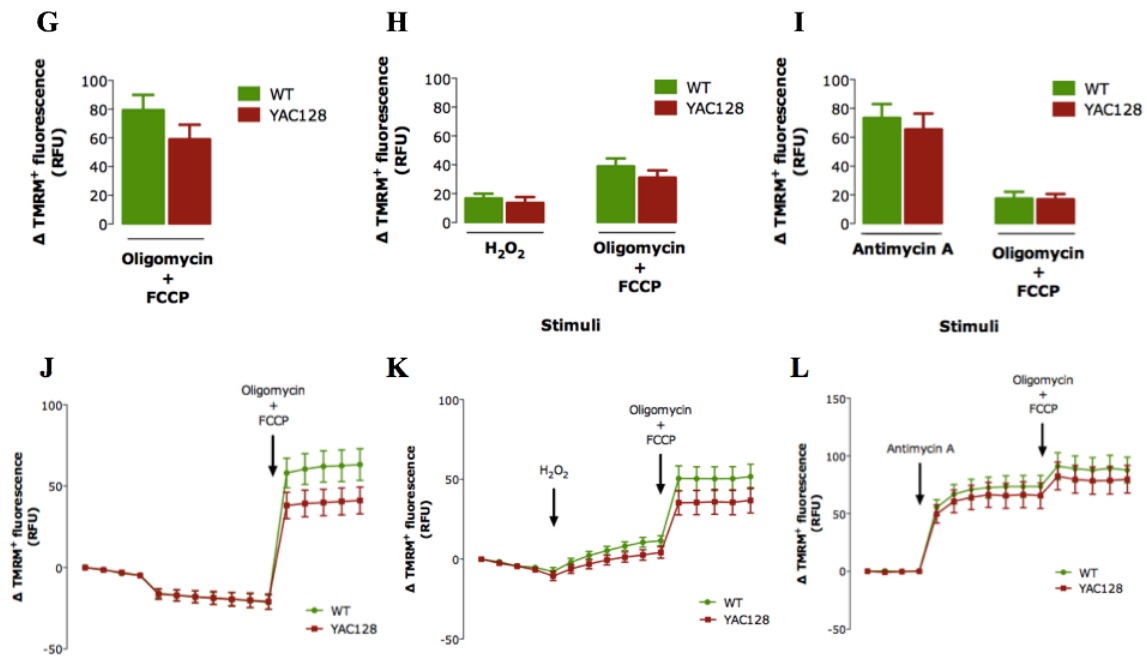


Figure 4. No alterations in mitochondrial membrane potential of wild-type and YAC128 synaptosomes. TMRM⁺ fluorescence was recorded in wild-type and YAC 128 cortical synaptosomes from mice with 9 (A, B, C, D, E, F) or 12 (G, H, I, J, K, L) months. Complete mitochondrial membrane depolarization was achieved by addition of 2 μ M FCCP plus 2 μ g/ml oligomycin (A, D, G, J) without or with prior stimulus with 2 μ M antimycin A (C, F, I, L) or 1 mM H₂O₂ (B, E, H, K). Results were expressed as the difference between the increase of TMRM⁺ fluorescence after the stimulus and the fluorescence values just prior to the stimulation (A, B, C, G, H, I). Graphs are representative registers of synaptosomal mitochondrial potential through time, during the experiments (D, E, F, J, K, L). Data are the mean \pm S.E.M. of 4 independent experiments performed in triplicates to quadruplicates

At 12 months, YAC128 synaptosomes seem to have a reduction in mitochondrial potential in comparison to the wild-type, however this tendency does not achieve statistical significance (Fig 4G). As previously observed for intrasynaptosomal Ca^{2+} levels, 1mM H_2O_2 and 2 μM antimycin A induced an increase in TMRM⁺ signal, and therefore, a reduction in mitochondrial potential of wild-type and YAC128 synaptosomes from 9- or 12-months mice (Fig 4E, 4F, 4K, 4L). Antimycin A produced an higher effect, probably due to its direct action in the mitochondrial respiratory chain, which is responsible for the maintenance of the mitochondrial potential (Fig. 4F, 4L). However, no differences were observed in the mitochondrial potentials between wild-type and YAC128 cortical synaptosomes, in response to H_2O_2 or antimycin A stimuli, at any age tested (Fig 4B-D, 4H).

Wild-type and YAC128 cortical synaptosomes show no differences in oxygen consumption

The evaluation of intrasynaptosomal Ca^{2+} levels and mitochondrial potential did not find any differences between the responses of wild-type and YAC cortical synaptosomes, either at 9 or 12 months. Therefore, we further pursued the characterization of the mitochondrial function of our synaptosomal preparations by assessing their oxygen consumption in a Clark-type oxygraph. Cortical synaptosomes were freshly prepared from brains of wild-type or YAC128 mice with 9 or 12 months of age, assembled in the oxygraph and energized with glucose. The oxygen consumption of synaptosomes were analyzed at basal conditions for a few minutes, before the administration of 2 $\mu\text{g}/\text{ml}$ oligomycin, which inhibits ATP synthase and hyperpolarizes the mitochondria. Finally, 2 μM CCCP were added to completely depolarize the mitochondrial potential, triggering the mitochondrial respiratory chain to work at its maximum capacity rate.

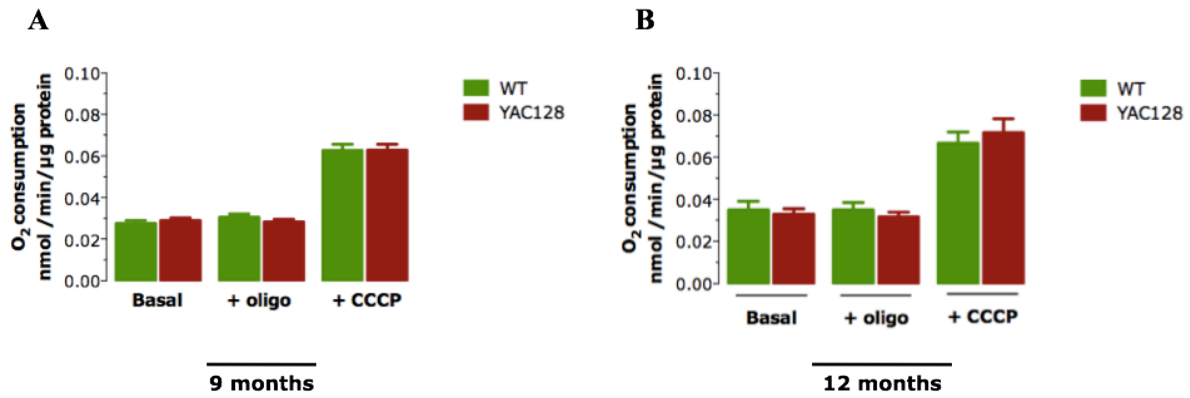


Figure 5. Wild-type and YAC128 synaptosomes have similar levels of O₂ consumption.

Cortical synaptosomes were isolated from brains of wild-type or YAC 128 transgenic mice with 9 months (A) or 12 months (B). The basal rate of O₂ consumption was recorded using an oxigraph, followed by sequential addition of 2 μg/ml oligomycin, 2 μM CCCP. Data are the mean ± S.E.M. of 4 independent experiments performed in triplicates to quadruplicates.

No differences in the oxygen consumption rates between wild-type and YAC128 synaptosomes were detected at any condition evaluated (Fig. 5). The basal rates were identical in both wild-type and transgenic synaptosomal preparations at either 9 or 12 months (Fig 5A, 5B). Oligomycin produced the same response in wild-type and YAC128 cortical synaptosomes and complete depolarization with CCCP revealed similar maximal oxygen consumption rates for both synaptosomal preparations at the two ages tested (Fig 5A, 5B). Overall, the mitochondrial respiratory chains of wild-type and YAC128 cortical synaptosomes seem to have no major differences in their metabolic capacities.

Brain mitochondria from 12-month YAC128 mice produce less H₂O₂ over time.

Analysis of synaptosomal preparations permitted an evaluation of the mitochondrial state of presynaptic mitochondria, since synaptosomes derive primarily from detached presynaptic terminals. To expand our studies beyond presynaptic mitochondria, we isolated brain mitochondria from cortices of wild-type and YAC128 mice with 12 months of age and used them to assess the same parameters previously evaluated in synaptosomes.

12 months

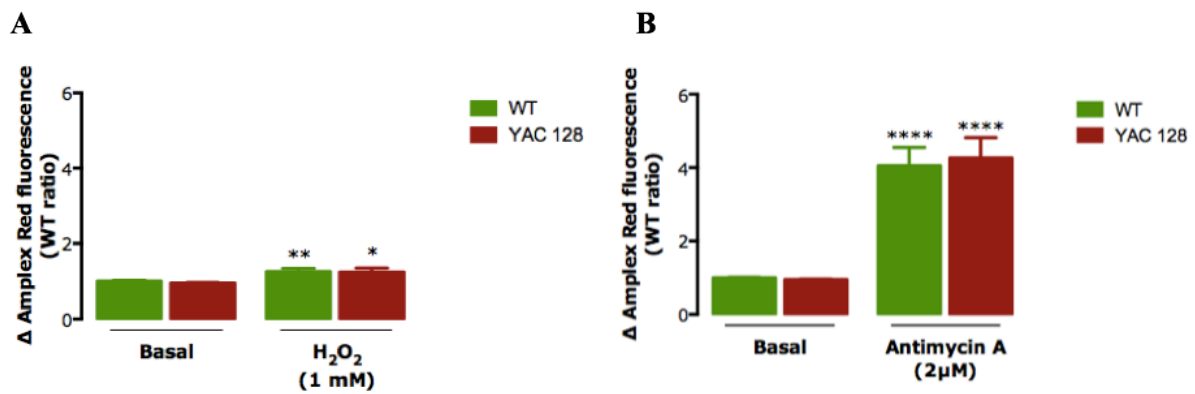


Figure 6. Isolated wild-type and HD cortical mitochondria produce equal levels of H₂O₂.

The production of H₂O₂ was measured in wild-type and YAC 128 cortical mitochondria from mice with 12 months of age. The increase in H₂O₂ levels was assessed under basal conditions (A, B), after a pre-incubation with 1 mM H₂O₂ (A) or a 2 μM antimycin A stimulus (B), through Amplex red fluorometry. Data are the mean ± S.E.M. of 4 independent experiments performed in triplicates to quadruplicates. Statistical analysis: *P<0.05, compared to YAC128 mitochondria under basal conditions, **P<0.01, compared to wild-type mitochondria under basal conditions, ****P<0.0001, compared to the respective mitochondria control (wild-type or YAC128) under basal conditions (two-way ANOVA, followed by Sidak's multiple comparisons test).

As previously done for synaptosomes, the measurement of H₂O₂ production was carried out fluometrically, following the increase in Amplex red fluorescence over time. Wild-type or YAC128 brain mitochondria produced the same amount of H₂O₂ at basal conditions, that is, in the absence of any prior challenging stimulus (Fig. 6A,B). Both the mitochondrial inhibition with 2 μM antimycin A inhibition and the 30 minute pre-incubation with 1 mM H₂O₂ induced statistically significant increases in H₂O₂ production in wild-type and YAC128 mitochondria (Fig. 6). Once again, antimycin A produced the most significant increases in H₂O₂ levels, however, wild-type and YAC128 mitochondria exhibited no differences in their H₂O₂ production in response to this mitochondrial inhibitor (Fig. 6B). H₂O₂ pre-incubation also promoted an higher rate of hydrogen production in wild-type and YAC128 brain mitochondria, yet this increase in H₂O₂ levels was similar in both populations of mitochondria, with no differences found between their rates of H₂O₂ production (Fig. 6A).

Wild-type and YAC128 brain mitochondria have no differences in their respiratory control ratio

After studying the H₂O₂ production, we further investigated if there were any alterations in mitochondrial energetic metabolism of wild-type or YAC128 brain mitochondria from 12-month old mice. The measurement of respiratory control ratio (RCR) is an estimation of coupling between the mitochondrial electron transport and ATP production. These reactions are independent and distinct from each other, but are usually tightly coupled. RCR is measured on the oxygraph, comparing the rates of oxygen consumption in the absence (state 4) and in the presence (state 3) of ADP. RCR corresponds to the ratio between these two rates (state 3/state 4).

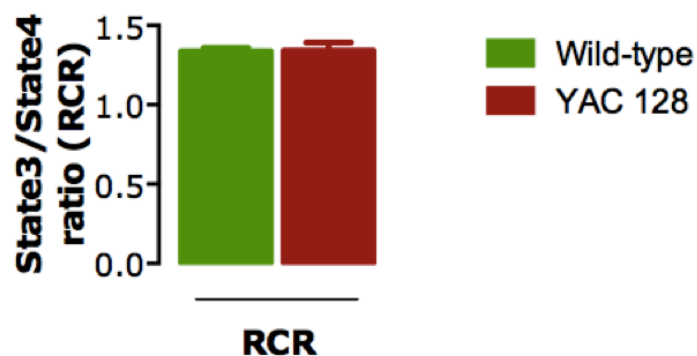


Figure 7. No differences in the respiratory control ratio (RCR) of wild-type and YAC128 cortical mitochondria.

Cortical mitochondria were isolated from brains of wild-type or YAC 128 transgenic mice with 12 months. The rate of O₂ consumption was recorded using an oxygraph apparatus, followed by sequential addition of 25 nM ADP, 2 μg/ml oligomycin, 2 μM CCCP. RCR was calculated through the ratio between the rates of oxygen consumption in the absence (state 4) and in the presence (state 3) of ADP. Data are the mean ± S.E.M. of 4 independent experiments performed in triplicates to quadruplicates.

Brain mitochondria were freshly isolated from cortices of wild-type and YAC128 mice with 12 months of age and analyzed in a oxygraph containing a Clark-type oxygen electrode. Initially, the mitochondria were energized with 3 mM succinate and the rate of oxygen consumption (state 4) was registered. Next, state 3 respiration was challenged by adding 25 nM ADP and the increase in oxygen consumption monitored. Interestingly, there were no

significant differences in the RCR of wild-type and YAC128 brain mitochondria, suggesting that a possible uncoupling mechanism between the mitochondrial respiration and phosphorylation could not account for by the difference in H₂O₂ production previously detected (Fig. 7).

Discussion

Oxidative stress has long been associated to HD neurodegeneration. Indications of increased ROS formation were found in human HD *post-mortem* cortex and striatum and increased levels of ROS production was confirmed in fibroblasts of HD patients and HD cybrids.^{30,31} Moreover, significant increases in nuclear and mitochondrial levels of 8-hydroxy-2'-deoxyguanosine adducts were observed in striatum, cortex, serum, leukocytes and plasma from HD patients, suggesting a higher grade of nucleotide oxidation.^{23,32-36} Lipid peroxidation by-products have also been shown to be elevated in brain tissue and bodily fluids of HD patients.^{33,37-40} Furthermore, oxidation of specific protein targets, including mitochondrial enzymes, has been detected in the striatum and cortex of HD patients and the oxidative alterations of these proteins were shown to decrease their catalytic activity.^{41,48} Therefore, it would be expected to find some level of oxidative stress in our HD animal model, the YAC128 mice.

Indeed, YAC128 cortical synaptosomes from 12-month old mice exhibited an increase in H₂O₂ production at basal levels, without any stimulation. Interestingly, this increase in H₂O₂ levels in comparison to wild-type is not observed at 9-months old synaptosomes, suggesting that later stages of disease and HD progression in YAC128 mice may be associated with augmented ROS production. Moreover, YAC128 synaptosomes seem to be more susceptible to an oxidative-enriched environment than their wild-type counterparts, since a pre-incubation with H₂O₂ promoted a significant increase in H₂O₂ production at both ages tested. On the other hand, wild-type synaptosomes were not susceptible to H₂O₂ pre-incubation, since they exhibited levels of H₂O₂ production similar to unstimulated synaptosomes. Therefore, YAC128 synaptosomes might have a reduction in the defenses to oxidative stress, which become overloaded by the pre-incubation with H₂O₂, leading to an accumulation and an increase in H₂O₂ endogenously produced. Wild-type synaptosomes kept their antioxidant defenses preserved and seem to be able to dwell under a oxidative stimulus. It would be

important to measure the levels and the activity of antioxidant pathways in our synaptosomal preparations to clarify this higher susceptibility of YAC128 synaptosomes to H₂O₂ pre-incubation. Moreover, the deficit in antioxidant defenses seems to be present early in the disease, as synaptosomes from both 9 and 12 month-old YAC128 mice exhibited the same susceptibility to H₂O₂ pre-incubation. Therefore, synaptosomes from early ages have to be isolated and tested to verify how soon in disease progression the susceptibility to an oxidative environment becomes apparent or if it is a characteristic inherent to the HD state. Previous studies support this reduction in antioxidant defenses in HD. A degradation of the antioxidant systems have been detected in plasma and erythrocytes from HD patients.²³ Furthermore, the levels of reduced glutathione seem to be lower in plasma of HD patients⁴⁴ and oxidized glutathione levels were also found to be decreased in the striatum of HD patients.⁴⁹

Antimycin A inhibition promoted a more robust and consistent increase in H₂O₂ production in comparison to H₂O₂ pre-incubation, in both wild-type and YAC128 synaptosomes. The production of a similar effect in wild-type and YAC128 synaptosomes may be due to the mechanism through which antimycin A increases the H₂O₂ levels, a direct mitochondrial complex inhibition. Through direct inhibition of the mitochondrial respiratory chain, antimycin A disrupts the normal flow of electrons through the mitochondrial complexes, increasing the electron leakage and the formation of ROS. Therefore, antimycin A acts by directly increasing the levels of ROS (H₂O₂ included) and not through a reduction in oxidative defenses. This mechanism might explain why there were no differences in H₂O₂ production levels between wild-type and YAC128 synaptosomes under antimycin A inhibition, because both wild-type and YAC128 synaptosomes seem to have a equally functional mitochondrial respiratory chain, and therefore, may share similar capacities to produced ROS under mitochondrial inhibition. The effect of antimycin A at inducing H₂O₂ production might be so robust that overloads the antioxidant defenses of both wild-type and YAC128 synaptosomes,

overshadowing the difference previously observed after H₂O₂ pre-incubation. Once more, further experiments will have to be carried out to support this hypothesis.

Wild-type and YAC128 cortical synaptosomes from mice with 9 or 12 months old proved to be not different in most of the mitochondrial parameters evaluated, supporting the idea that, in general, wild-type and YAC128 mitochondria are similarly functional and YAC128 synaptosomes do not carry a major alteration in mitochondrial function. Truly, YAC128 exhibited equal intrasynaptosomal Ca²⁺ levels, mitochondrial membrane potential and oxygen consumption rates than wild-type synaptosomes, at any age tested and under basal or stimulated conditions. These results add more support to the hypothesis that the increases in H₂O₂ production observed in YAC synaptosomes are a consequence of decreased antioxidant defenses and not to dysfunctional mitochondria. However, previous works have found differences between wild-type and HD models in many of the mitochondrial parameters that we have tested.²⁰⁻²⁹ One possible explanation for this discrepancy might have to be with the usage of cortical instead of striatal synaptosomes. Although the cortex is also affected in HD, it happens at later stages of the disease, while striatum is the primary degenerating brain area.

Surprisingly, isolated wild-type and YAC128 cortical mitochondria continued to exhibit similar functional activities as proven by the absence of differences between their RCRs, however the higher susceptibility of YAC128 mitochondria to H₂O₂ pre-incubation was no longer observed, when outside of a synaptosomal environment. Indeed, antimycin A continued to induce the higher and robust increases in H₂O₂ levels in both mitochondrial populations, as previously observed in synaptosomes. However, H₂O₂ pre-incubation induced identical increases in wild-type and YAC128 mitochondria. Literally, what seems to be occurring is a novel augmented susceptibility of wild-type mitochondria to H₂O₂ pre-incubation to the same levels shown by YAC128 mitochondria, since before, H₂O₂-treated wild-type synaptosomes exhibited H₂O₂ levels similar to the basal conditions. Isolated mitochondria may be deprived of the antioxidant defenses which allow wild-type

synaptosomes to deal with the oxidative stimulus. Therefore, in the absence of these defenses, wild-type and YAC128 mitochondria begin to respond similarly to the H₂O₂ pre-incubation. These results might indicate that the presumable deficiency in antioxidant defenses in YAC128 are not intrinsic to mitochondria but are present in the synaptosomes. Indeed, a major enzyme involved in the decomposition of H₂O₂, catalase, is not located in mitochondria but primarily in other intracellular organelles, the peroxisomes.⁵⁰ In fact, a significant reduction in catalase activity was found in skin fibroblasts and erythrocytes of HD patients.^{43,}

51

In conclusion, our data suggest an association between HD progression and an increase in H₂O₂ levels, which seems not to be a consequence of a dysfunctional mitochondrial respiratory chain, but rather due to a probable deficiency in antioxidant defenses. However, more studies will have to be performed in order to clarify this hypothesis.

Acknowledgments

À Professora Doutora Ana Cristina Rego por me ter aceitado e orientado em mais uma tese. Tem sido um prazer aprender e crescer cientificamente dentro do seu grupo e debaixo da sua visão e conhecimento.

Aos meus colegas de trabalho, a todos sem exceção, aos presentes e aos que já saíram do laboratório para perseguirem as suas novas questões científicas. Um obrigado especial à Sandra e à Luísa, por me ajudarem nas experiências apresentadas neste trabalho.

Aos meus colegas do Mestrado Integrado em Medicina, a classe 2009-2015, porque partilhámos toda uma caminhada extraordinária, em conjunto.

Aos alunos do concurso de licenciados por comungarem comigo da loucura de iniciar um projeto tão longo, tão trabalhoso, numa altura de vida menos propícia a aventuras, mas que no final, nos traz tanta recompensa. Em particular, devolvo um carinho especial à Marta, à Sara, à Catarina e à Sandra com quem partilhei as ansiedades, as preocupações, as dúvidas, o nervosismo antes das orais, mas também e principalmente, as piadas, os risos e a alegria.

Aos meus amigos, Gil, Armanda, Max, Rúben, Regina, Rui, Magda, Luís, André, Carlos; entre muitos outros, que souberam compreender as minhas constantes ausências porque havia estudo, porque havia orais, mas ainda assim portadores da paciência para ouvir as minhas queixas, as minhas lamúrias e darem-me incentivo para continuar, sempre um pouco mais.

À minha mãe e ao meu pai, por quase tudo. Pelo apoio e compreensão sem limites, pela amizade estável, inabalável. Ao realizar-me, sinto que os realizo também, e dessa forma, nada me dá mais orgulho, que terminar este percurso com eles.

Esta tese é para todos vós.

References

1. Evans, S. J., Douglas, I., Rawlins, M. D., Wexler, N. S., Tabrizi, S. J. and Smeeth, L. (2013). Prevalence of adult Huntington's disease in the UK based on diagnoses recorded in general practice records. *Journal of neurology, neurosurgery, and psychiatry* 84(10), 1156-60
2. Pringsheim, T., Wiltshire, K., Day, L., Dykeman, J., Steeves, T. and Jette, N. (2012). The incidence and prevalence of Huntington's disease: a systematic review and meta-analysis. *Movement disorders : official journal of the Movement Disorder Society* 27(9), 1083-91
3. Warby, S. C., Visscher, H., Collins, J. A., Doty, C. N., Carter, C., Butland, S. L., Hayden, A. R., Kanazawa, I., Ross, C. J. and Hayden, M. R. (2011). HTT haplotypes contribute to differences in Huntington disease prevalence between Europe and East Asia. *European journal of human genetics : EJHG* 19(5), 561-6
4. Vonsattel, J. P. and DiFiglia, M. (1998). Huntington disease. *Journal of neuropathology and experimental neurology* 57(5), 369-84
5. Van Raamsdonk, J. M., Murphy, Z., Slow, E. J., Leavitt, B. R. and Hayden, M. R. (2005). Selective degeneration and nuclear localization of mutant huntingtin in the YAC128 mouse model of Huntington disease. *Human molecular genetics* 14(24), 3823-35
6. Caine, E. D. and Shoulson, I. (1983). Psychiatric syndromes in Huntington's disease. *The American journal of psychiatry* 140(6), 728-33
7. Paulsen, J. S., Ready, R. E., Hamilton, J. M., Mega, M. S. and Cummings, J. L. (2001). Neuropsychiatric aspects of Huntington's disease. *Journal of neurology, neurosurgery, and psychiatry* 71(3), 310-4
8. Josiassen, R. C., Curry, L. M. and Mancall, E. L. (1983). Development of neuropsychological deficits in Huntington's disease. *Archives of neurology* 40(13), 791-6
9. Duff, K., Paulsen, J. S., Beglinger, L. J., Langbehn, D. R., Stout, J. C. and Predict, H. D. I. o. t. H. S. G. (2007). Psychiatric symptoms in Huntington's disease before diagnosis: the predict-HD study. *Biological psychiatry* 62(12), 1341-6
10. Kirkwood, S. C., Siemers, E., Viken, R., Hodes, M. E., Conneally, P. M., Christian, J. C. and Foroud, T. (2002). Longitudinal personality changes among presymptomatic Huntington disease gene carriers. *Neuropsychiatry, neuropsychology, and behavioral neurology* 15(3), 192-7
11. Berardelli, A., Noth, J., Thompson, P. D., Bollen, E. L., Curra, A., Deuschl, G., van Dijk, J. G., Topper, R., Schwarz, M. and Roos, R. A. (1999). Pathophysiology of chorea and bradykinesia in Huntington's disease. *Movement disorders : official journal of the Movement Disorder Society* 14(3), 398-403
12. Penney, J. B., Jr., Young, A. B., Shoulson, I., Starosta-Rubenstein, S., Snodgrass, S. R., Sanchez-Ramos, J., Ramos-Arroyo, M., Gomez, F., Penchaszadeh, G., Alvir, J. and et al. (1990). Huntington's disease in Venezuela: 7 years of follow-up on symptomatic and asymptomatic individuals. *Movement disorders : official journal of the Movement Disorder Society* 5(2), 93-9
13. Louis, E. D., Anderson, K. E., Moskowitz, C., Thorne, D. Z. and Marder, K. (2000). Dystonia-predominant adult-onset Huntington disease: association between motor phenotype and age of onset in adults. *Archives of neurology* 57(9), 1326-30
14. Aylward, E. H. (2007). Change in MRI striatal volumes as a biomarker in preclinical Huntington's disease. *Brain research bulletin* 72(2-3), 152-8

15. Montoya, A., Price, B. H., Menear, M. and Lepage, M. (2006). Brain imaging and cognitive dysfunctions in Huntington's disease. *Journal of psychiatry & neuroscience : JPN* 31(1), 21-9
16. Folstein S.E., Folstein M.F. (1983). Psychiatric features of Huntington's disease: recent approaches and findings. *Psychiatr Dev.* 1,193-205
17. Walker, F. O. (2007). Huntington's disease. *Lancet* 369(9557), 218-28
18. Gusella, J. F., Wexler, N. S., Conneally, P. M., Naylor, S. L., Anderson, M. A., Tanzi, R. E., Watkins, P. C., Ottina, K., Wallace, M. R., Sakaguchi, A. Y. and et al. (1983). A polymorphic DNA marker genetically linked to Huntington's disease. *Nature* 306(5940), 234-8
19. Warby, S. C., Montpetit, A., Hayden, A. R., Carroll, J. B., Butland, S. L., Visscher, H., Collins, J. A., Semaka, A., Hudson, T. J. and Hayden, M. R. (2009). CAG expansion in the Huntington disease gene is associated with a specific and targetable predisposing haplogroup. *American journal of human genetics* 84(3), 351-66
20. Bae, B. I., Xu, H., Igarashi, S., Fujimuro, M., Agrawal, N., Taya, Y., Hayward, S. D., Moran, T. H., Montell, C., Ross, C. A., Snyder, S. H. and Sawa, A. (2005). p53 mediates cellular dysfunction and behavioral abnormalities in Huntington's disease. *Neuron* 47(1), 29-41
21. Tang, T.S., Slow, E., Lupu, V., Stavrovskaya, I.G., Sugimori, M., et al. (2005). Disturbed Ca²⁺ signaling and apoptosis of medium spiny neurons in Huntington's disease. *Proc. Natl. Acad. Sci. USA* 102, 2602-2607
22. Browne, S.E., Beal, M.F. (2006). Oxidative damage in Huntington's disease pathogenesis. *Antioxid. Redox Signal.* 8, 2061-2073
23. Túnes, I., Sánchez-López, F., Agüera, E., Fernández-Bolaños, R., Sánchez, F.M., Tasset-Cuevas, I. (2011). Important role of oxidative stress biomarkers in Huntington's disease. *J. Med. Chem.* 54, 5602-5606
24. Quintanilla R.A., Johnson G.V. (2009). Role of mitochondrial dysfunction in the pathogenesis of Huntington's disease. *Brain Res. Bull.* 80, 242-247
25. Pickrell, A. M., Fukui, H., Wang, X., Pinto, M. and Moraes, C. T. (2011). The striatum is highly susceptible to mitochondrial oxidative phosphorylation dysfunctions. *The Journal of neuroscience : the official journal of the Society for Neuroscience* 31(27), 9895-904
26. Beal M.F., Brouillet E., Jenkins B., Henshaw R., Rosen B., Hyman B.T. (1993). Age-dependent striatal excitotoxic lesions produced by the endogenous mitochondrial inhibitor malonate. *J. Neurochem.* 61, 1147-1150
27. Oliveira J.M., Chen S., Almeida S., Riley R., Gonçalves J., et al. (2006). Mitochondrial-dependent Ca²⁺ handling in Huntington's disease striatal cells: effect of histone deacetylase inhibitors. *J Neurosci.* 26,11174-11186
28. Panov, A.V., Gutekunst, C.A., Leavitt, B.R., Hayden, M.R., Burke, J.R., et al. (2002). Early mitochondrial calcium defects in Huntington's disease are a direct effect of polyglutamines. *Nat. Neurosci.* 5, 731-736
29. Puranam K.L., Wu G., Strittmatter W.J., Burke J.R. (2006). Polyglutamine expansion inhibits respiration by increasing reactive oxygen species in isolated mitochondria. *Biochem. Biophys. Res. Commun.* 341, 607-613
30. Wang, J. Q., Chen, Q., Wang, X., Wang, Q. C., Wang, Y., Cheng, H. P., Guo, C., Sun, Q., Chen, Q. and Tang, T. S. (2013). Dysregulation of mitochondrial calcium signaling and superoxide flashes cause mitochondrial genomic DNA damage in Huntington disease. *The Journal of biological chemistry* 288(5), 3070-84
31. Ferreira, I. L., Nascimento, M. V., Ribeiro, M., Almeida, S., Cardoso, S. M., Grazina, M., Pratas, J., Santos, M. J., Janeiro, C., Oliveira, C. R. and Rego, A. C. (2010).

- Mitochondrial-dependent apoptosis in Huntington's disease human cybrids. *Experimental neurology* 222(2), 243-55
32. Browne, S. E., Bowling, A. C., MacGarvey, U., Baik, M. J., Berger, S. C., Muqit, M. M., Bird, E. D. and Beal, M. F. (1997). Oxidative damage and metabolic dysfunction in Huntington's disease: selective vulnerability of the basal ganglia. *Annals of neurology* 41(5), 646-53
 33. Chen, C. M., Wu, Y. R., Cheng, M. L., Liu, J. L., Lee, Y. M., Lee, P. W., Soong, B. W. and Chiu, D. T. (2007). Increased oxidative damage and mitochondrial abnormalities in the peripheral blood of Huntington's disease patients. *Biochemical and biophysical research communications* 359(2), 335-40
 34. Polidori, M. C., Mecocci, P., Browne, S. E., Senin, U. and Beal, M. F. (1999). Oxidative damage to mitochondrial DNA in Huntington's disease parietal cortex. *Neuroscience letters* 272(1), 53-6
 35. Shirendeb, U., Reddy, A. P., Manczak, M., Calkins, M. J., Mao, P., Tagle, D. A. and Reddy, P. H. (2011). Abnormal mitochondrial dynamics, mitochondrial loss and mutant huntingtin oligomers in Huntington's disease: implications for selective neuronal damage. *Human molecular genetics* 20(7), 1438-55
 36. Hersch, S. M., Gevorkian, S., Marder, K., Moskowitz, C., Feigin, A., Cox, M., Como, P., Zimmerman, C., Lin, M., Zhang, L., Ulug, A. M., Beal, M. F., Matson, W., Bogdanov, M., Ebbel, E., Zaleta, A., Kaneko, Y., Jenkins, B., Hevelone, N., Zhang, H., Yu, H., Schoenfeld, D., Ferrante, R. and Rosas, H. D. (2006). Creatine in Huntington disease is safe, tolerable, bioavailable in brain and reduces serum 8OH²dG. *Neurology* 66(2), 250-2
 37. Browne, S. E., Ferrante, R. J. and Beal, M. F. (1999). Oxidative stress in Huntington's disease. *Brain pathology* 9(1), 147-63
 38. Lee, J., Kosaras, B., Del Signore, S. J., Cormier, K., McKee, A., Ratan, R. R., Kowall, N. W. and Ryu, H. (2011). Modulation of lipid peroxidation and mitochondrial function improves neuropathology in Huntington's disease mice. *Acta neuropathologica* 121(4), 487-98
 39. Montine, T. J., Beal, M. F., Robertson, D., Cudkowicz, M. E., Biaggioni, I., O'Donnell, H., Zackert, W. E., Roberts, L. J. and Morrow, J. D. (1999). Cerebrospinal fluid F₂-isoprostanes are elevated in Huntington's disease. *Neurology* 52(5), 1104-5
 40. Stoy, N., Mackay, G. M., Forrest, C. M., Christofides, J., Egerton, M., Stone, T. W. and Darlington, L. G. (2005). Tryptophan metabolism and oxidative stress in patients with Huntington's disease. *Journal of neurochemistry* 93(3), 611-23
 41. Sorolla, M. A., Rodriguez-Colman, M. J., Tamarit, J., Ortega, Z., Lucas, J. J., Ferrer, I., Ros, J. and Cabisco, E. (2010). Protein oxidation in Huntington disease affects energy production and vitamin B6 metabolism. *Free radical biology & medicine* 49(4), 612-21
 42. Beal, M. F. (1992). Does impairment of energy metabolism result in excitotoxic neuronal death in neurodegenerative illnesses? *Annals of neurology* 31(2), 119-30
 43. Zanella, A., Izzo, C., Meola, G., Mariani, M., Colotti, M. T., Silani, V., Pellegata, G. and Scarlato, G. (1980). Metabolic impairment and membrane abnormality in red cells from Huntington's disease. *Journal of the neurological sciences* 47(1), 93-103
 44. Klepac, N., Relja, M., Klepac, R., Hecimovic, S., Babic, T. and Trkulja, V. (2007). Oxidative stress parameters in plasma of Huntington's disease patients, asymptomatic Huntington's disease gene carriers and healthy subjects : a cross-sectional study. *Journal of neurology* 254(12), 1676-83
 45. Slow, E. J., van Raamsdonk, J., Rogers, D., Coleman, S. H., Graham, R. K., Deng, Y., Oh, R., Bissada, N., Hossain, S. M., Yang, Y. Z., Li, X. J., Simpson, E. M., Gutekunst, C. A., Leavitt, B. R. and Hayden, M. R. (2003). Selective striatal neuronal loss in a

- YAC128 mouse model of Huntington disease. *Human molecular genetics* 12(13), 1555-67
46. Rodrigues, R. J., Almeida, T., Richardson, P. J., Oliveira, C. R., Cunha, R.A. (2005). Dual presynaptic control by ATP of glutamate release via facilitatory P2X₁, P2X_{2/3}, P2X₃ and inhibitory P2Y₁, P2Y₂, and/or P2Y₄ receptors in the rat hippocampus. *The journal of neuroscience* 25(27), 6286-95
 47. Wang, X., Leverin, A., Han, W., Zhu, C., Johansson, B. R., Jacotot, E., Ten, V. S., Sims, N. R., Hagberg, H. (2011). Isolation of brain mitochondria from neonatal mice. *Journal of neurochemistry* 119, 1253-61
 48. Sorolla, M. A., Reverter-Branchat, G., Tamarit, J., Ferrer, I., Ros, J. and Cabiscol, E. (2008). Proteomic and oxidative stress analysis in human brain samples of Huntington disease. *Free radical biology & medicine* 45(5), 667-78
 49. Sian, J., Dexter, D. T., Lees, A. J., Daniel, S., Agid, Y., Javoy-Agid, F., Jenner, P. and Marsden, C. D. (1994). Alterations in glutathione levels in Parkinson's disease and other neurodegenerative disorders affecting basal ganglia. *Annals of neurology* 36(3), 348-55
 50. Murakami, K., Ichinohe, Y., Koike, M., Sasaoka, N., Iemura, S., Natsume, T., Kakizuka, A. (2013). *PLoS One* 8(2), e56012
 51. del Hoyo, P., Garcia-Redondo, A., de Bustos, F., Molina, J. A., Sayed, Y., Alonso-Navarro, H., Caballero, L., Arenas, J. and Jimenez-Jimenez, F. J. (2006). Oxidative stress in skin fibroblasts cultures of patients with Huntington's disease. *Neurochemical research* 31(9), 1103-9